**Manuscript version: Author's Accepted Manuscript**

The version presented in WRAP is the author's accepted manuscript and may differ from the published version or Version of Record.

**Persistent WRAP URL:**

http://wrap.warwick.ac.uk/143009

**How to cite:**

Please refer to published version for the most recent bibliographic citation information.
If a published version is known of, the repository item page linked to above, will contain details on accessing it.

**Copyright and reuse:**

The Warwick Research Archive Portal (WRAP) makes this work by researchers of the University of Warwick available open access under the following conditions.

Copyright © and all moral rights to the version of the paper presented here belong to the individual author(s) and/or other copyright owners. To the extent reasonable and practicable the material made available in WRAP has been checked for eligibility before being made available.

Copies of full items can be used for personal research or study, educational, or not-for-profit purposes without prior permission or charge. Provided that the authors, title and full bibliographic details are credited, a hyperlink and/or URL is given for the original metadata page and the content is not changed in any way.

**Publisher's statement:**

Please refer to the repository item page, publisher's statement section, for further information.

For more information, please contact the WRAP Team at: wrap@warwick.ac.uk.

Title: High performance $Na_{0.5}[Ni_{0.23}Fe_{0.13}Mn_{0.63}]O_2$ cathode for sodium-ion battery

*Ivana Hasa, Daniel Buchholz, Stefano Passerini[*], Bruno Scrosati and Jusef Hassoun[*]*

I. Hasa, Dr. J. Hassoun,
Department of Chemistry, University of Rome, Sapienza, Piazzale Aldo Moro, 5, 00185
Rome, Italy
E-mail: jusef.hassoun@uniroma1.it
D. Buchholz, Prof. S. Passerini
Institute of Physical Chemistry, University of Muenster, Corrensstrasse 28, 48149, Muenster,
Germany
Prof. S. Passerini
Helmholtz Institute Ulm, Karlsruhe Institute of Technology, Albert Einstein Allee11, 89081
Ulm, Germany
E-mail: stefano.passerini@uni-muenster.de
B. Scrosati
Italian Institute of Technology, Genova, Italy

**Abstract**

The synthesis of a new layered cathode material, $Na_{0.5}[Ni_{0.23}Fe_{0.13}Mn_{0.63}]O_2$, and its

characterization in terms of crystalline structure and electrochemical performance in a sodium

cell, is reported. X-ray diffraction studies and high resolution SEM images reveal a well-

defined P2-type layered structure, while the electrochemical tests evidence excellent

characteristics in terms of high capacity, extending up to 200 mAh $g^{-1}$, and cycle life, up to 70

cycles. This performance, in addition to the low cost and environmental compatibility of its

component, poses $Na_{0.5}[Ni_{0.23}Fe_{0.13}Mn_{0.63}]O_2$ among the best promising materials for the next

generation of sodium ion batteries.

1. Introduction

Presently, lithium-ion batteries (LIBs) are the most widespread rechargeable batteries

in the consumer electronic and portable device markets because of their unique properties. [1,2]

1

Due to their high energy density, LIBs are already considered in the transportation field and used to power hybrid (HEVs), plug-in hybrid (PHEVs) and full electric vehicles (EVs).[3] However, the increased demand of lithium and the comparably limited geographic location of resources is reflecting in a rapid rise of its price.[4,5] As a consequence, the identification of energy storage systems alternative to lithium is now seen as a valid step to lead to the development of economically sustainable secondary batteries. Among these, sodium-based batteries appear as very promising candidates due to the low cost and high abundance of sodium (the 4th most abundant element in the Earth crust), as well as the compatibility with aqueous electrolytes and anodic aluminum current collectors.[6-8]

Sodium has an ionic radius larger than lithium (1.06 Å *vs* 0.76 Å, respectively), preferring 6-fold coordination in octahedral or prismatic sites. This results in the confinement of the Na-based cathode structures into two big classes, i.e. poly-anionic networks and layered compounds.

Layered materials, characterized by $MO_6$ edge-sharing octahedral units forming $(MO_2)_n$ sheets, can easily host alkali atoms, such as sodium, within octahedral (O), tetrahedral (T, not favored) or prismatic (P) environments. Delmas *et al.* [9] classified these layered oxide materials into two main groups, differing by the alkali-ion intercalation site, i.e.: i) O-type layered materials that host the ions in octahedral sites and ii) P-type materials that accommodate the alkali ions in prismatic sites. In particular, sodium ions can lead to further distinct structures, i.e. O3, P2 and P3, where the number indicates the number of transition metal layers in the repeating cell unit. Various layered oxides containing only one transition metal species, such as $Na_xCoO_2$,[10,11] $Na_xCrO_2$,[12] $Na_xFeO_2$,[13,14] $Na_xMnO_2$[15] and $Na_xNiO_2$,[16] have been studied during the last years as reversible insertion cathodes for Na ions, however, with limited capacity and rate capability. Substituted sodium layered oxide, characterized by the contemporary presence of various transition metals in the electrode structure, are also suitable candidates to be used as sodium battery cathodes. Komaba *et al.* [17]

reported O3-type $Na_xNi_{0.5}Mn_{0.5}O_2$, showing a discharge capacity of 125 mAh·g$^{-1}$ when cycled in the 2.2 - 3.8 V voltage range at a rate of C/50. Nevertheless, a large capacity decay after only ten cycles was observed for this material upon cycling within the 2.0-4.5V voltage range (initial delivering a capacity about 185 mAh·g$^{-1}$). Hassoun *et al.* reported the characteristics and performance of a sodium-ion battery based on the Sn-C anode and O3-type $Na(Ni_{0.5}Mn_{0.5})O_2$ cathode. Operating with an average voltage of 2.8 V, this cell showed a specific capacity of 120 mAh·g$^{-1}$ and a cycle life extending to 50 cycles.[18] Dahn *et al.*[19] and Carlier *et al.* [20] demonstrated the suitability of P2-type $Na_{2/3}Ni_{1/3}Mn_{2/3}O_2$ as positive electrode for sodium batteries, reporting few cycles with delivered capacities ranging from 115 mAh·g$^{-1}$ to 160 mAh·g$^{-1}$. Meng and co-workers[21] extended the cycle number and demonstrated that the cell performance is affected by the P2-O2 phase transition occurring around 4.2V. Tarascon et al. proposed the O3-type $Na[Ni_{0.33}\ Mn_{0.33}Co_{0.33}]O_2$ electrode, demonstrating its ability to reversibly intercalate 0.5 eq. of Na leading to a capacity of 120 mAh·g$^{-1}$, [22] while Passerini and coworkers reported a cobalt-containing, Na-ion intercalation material, $Na_{0.45}Ni_{0.22}Co_{0.11}Mn_{0.66}O_2$ (space group P63/mmc), characterized by a specific capacity of 135 mAh·g$^{-1}$ and a cycle life prolonged up to 250 cycles[23,24] in conventional electrolytes, and around 200 mAh·g$^{-1}$ with a cycle life above 100 cycles in ionic liquid-based electrolytes.

The above review of the literature work on sodium-based layered oxides evidences that P2-type electrode materials are generally characterized by high capacity for a limited number of cycles, while O3-type electrodes deliver lower capacity but with extended cycle life. A comparative study between layered $Na_{2/3}[Fe_{1/2}Mn_{1/2}]O_2$ of the P2- and O3- type, reported by Komaba et al. [25], demonstrated, in fact, that the O3-type oxide is able to deliver a stable capacity of about 100 mAh·g$^{-1}$, while reversible capacity of 190 mAh·g$^{-1}$ is initially delivered by the P2-type oxide, however, with capacity retention of about 79% upon 30 charge-discharge cycles. Furthermore, Slater and coworkers [26] proposed the use of

Na[Ni$_{0.33}$Fe$_{0.33}$Mn$_{0.33}$]O$_2$ of O3-type as long-life electrode, extending to 150 cycles, in a full Na-ion cell, however, with a capacity limited to only 100 mAh·g$^{-1}$. These two latter works focused on the use of iron and manganese based oxides, which, due to their natural abundance and environmental and safety friendliness, are considered very suitable cathode materials for battery cost reduction. Moreover, P2-type, mixed iron and manganese oxides have demonstrated structural stability and improved electrochemical performances in terms of delivered reversible capacity. So far, however, the Jahn-Teller distortion, due to excess of Mn, has represented the key factor limiting the structural stability of the layered metal oxides upon sodium ion insertion. A general approach adopted to address this issue is the introduction of different metals in order to decrease the Mn(III) content and stabilize the overall crystal structure.

Following this trend, we focused the attention on a high capacity, P2-type electrode synthesized by a co-precipitation technique followed by thermal treatment and water rinsing.[23] The material, having a chemical composition of Na$_{0.5}$[Ni$_{0.23}$Fe$_{0.13}$Mn$_{0.63}$]O$_2$ and layered structure, revealed excellent performances in terms of high capacity, i.e. of about 200 mAh g$^{-1}$, and of long cycle life in conventional electrolytes. The results here reported evidence an effective improvement of the electrochemical properties of the electrode if compared with those already described in the literature, this being due to the contemporary presence of Mn, Ni and Fe in the crystal structure of the layered material.

2. Result and discussion

In this work we synthesized a P2-type layered material and characterized it as a cathode in sodium cells. A key role in the obtainment of this material is played by the sodium amount used for the synthesis, due to its crucial role in determining the structure of the final material. Excessive sodium amount, typical of the O3-type layered structure, was avoided. Sodium losses expected to occur during the annealing process in air (leading to the formation

4

of sodium carbonate and oxide), was counterbalanced by adding an extra amount (one equivalent) of NaOH, to the material precursors during synthesis. The rinsing process in aqueous solution[23,27] was used to remove the sodium carbonate and oxide.[22] In addition, this latter step grants the removal of Mn-based impurities formed during the synthesis steps, as, in fact, demonstrated by the ICP analysis of the water used for the rinsing step, which shows traces of Mn and Na.[27] Indeed, the stoichiometry of the rinsed compound, as detected by ICP, was $Na_{0.5}[Ni_{0.23}Fe_{0.13}Mn_{0.63}]O_2$. The same analysis performed on the pristine material after the annealing step evidenced a Na:Ni:Fe:Mn = 1:0.23:0.13:0.68 ratio, thus indicating that the rinsing process leads to the dissolution of residual sodium and manganese carbonates formed during the synthesis process, i.e. 0.25 mol of $Na_2CO_3$ and 0.05 mol of $Mn(CO_3)_2$.[22] Furthermore, the lower sodium content and defective transition metal ratio, i.e., 0.5 instead of 1, in the general formula $Na_{0.5}[Ni_{0.23}Fe_{0.13}Mn_{0.63}]O_2$ of the rinsed material can be attributed to sodium-proton exchange as well as Ni(II)/Ni(III) oxidation upon water rinsing. This defective formulation effectively leads to the presence of vacancies that is generally reflected in a phase stabilization of the material.[28-30]

Considering the synthesis conditions (high temperature in open air) and the literature data, the oxidation states of the transition metals in the compound are assumed to be two and three for Ni(II/III), three for Fe(III) and four for Mn(IV).

Figure 1

**Figure 1** reports a summary of the characteristics of the pristine and rinsed materials in terms of structure, morphology and electrochemical response in sodium cell. The XRD diffraction patterns of Figures 1a and b, indexed by using the reference ICSD-93469, demonstrate that both materials (pristine and rinsed) have a layered P2 structure belonging to the hexagonal $P6_3/mmc$ space group (internal reference number 194). Furthermore, the pristine material shows some additional peaks (indicated by asterisks in the figure)

attributable to the above-mentioned impurities (water soluble carbonates) since they disappear upon rinsing (Fig. 1b).

The SEM images of Figure 1c clearly evidence that the pristine material surface (Fig.1c) is covered by impurities, which are almost completely removed by the rinsing process (see Fig. 1d). The rinsing step exposes the morphology typical of enhanced layered compounds, characterized by a sequence of smooth facets of about 500 nm size (see further images in SI, Fig. S1). Furthermore, the BET analysis of the materials shows that the pristine powder is characterized by a specific surface area of $0.303 \ m^2 \, g^{-1}$ that increases to $3.27 \ m^2 \, g^{-1}$ upon rinsing. The increased surface area is due to the cleaning of the material surface, in good agreement with the SEM images in Fig.1c and d. This is expected to result in an improved electrochemical behavior of the material due to the easier access of $Na^+$ ion within the layers, as indeed demonstrated in this work.

Figure 1e reports the cell voltage profiles as a function of the sodium content in the pristine material, recorded during the two, initial cycles. From the figure it is seen that 0.7 equivalents of sodium are involved during the first charge, while the sodium exchanged in the following discharge amounts to 0.8 equivalents. This behaviour, in addition to the different voltage profile observed during the first charge in respect to the following cycles, is most likely attributed to a structural reorganization of the material, the electrolyte oxidation with SEI layer formation, the sodium defective composition of the material, and the presence of impurities. In fact, the inset of figure 1e, reporting the amount of sodium reversibly exchanged upon cycles, shows that the pristine material is affected by a capacity fading, probably due to the presence of the above-mentioned carbonate and oxide impurities. The electrochemical behaviour of the rinsed material, reported in Figure 1f, reveals a relevant improvement of the voltage profile during the initial cycle, which becomes very similar to the profile of the following cycles. Also, a substantial decrease of the sodium involved in the first charge is observed, i.e. of about 0.4 equivalents, due to its lower content in the rinsed material.

However, during the following cycles, the exchanged amount of sodium upon a whole charge-discharge cycle increases up to 0.7 equivalents. As it is seen in the inset of Figure 1e, the (de-)sodiation process occurs with excellent reversibility and stability, thus further evidencing the beneficial role of the rinsing procedure.

Table 1

**Table 1** reports the lattice parameters, as obtained from the Rietveld refinement, of the pristine and rinsed materials. The table evidences an increase of the $c$ parameter (inter-layers) and a decrease of the $a$ parameter (intra-layer) upon rinsing, as expected by the reduction of the sodium content.[23] Indeed, the water treatment may eventually lead to the removal of sodium accompanied by simultaneous possible $Ni^{2+}$ to $Ni^{+3}$ oxidation with a consequent increase of the repulsion between the oxygen atoms belonging to subsequent layers, as well as a decrease of the M-M distance of the structural reorganized transition metals [20] in the layer. These changes are reflected by a slight shift of the XRD pattern of figure 1b of the (00l) and (10l) reflections toward lower angles and of the (110) and (112) reflections towards higher angles.

Figure 2

**Figure 2** illustrates the appearance of the rinsed material, as shown by the FE-SEM image, together with its structure, as obtained by the refined cell parameters of Table 1. As mentioned earlier in the Introduction, the sodium ions in $Na_{0.5}[Ni_{0.23}Fe_{0.13}Mn_{0.63}]O_2$ lie in between the transition metal layers and occupy two different prismatic sites, i.e., the Na(1) position, sharing faces with the $MO_6$ octahedra in the layers above and below, and the Na(2) position, sharing only edges. Accordingly, the FE-SEM image in figure 2 shows that the above-described structure is reflected in an extremely well-defined layered morphology with series of adherent planes forming a single particle.

Figure 3

**Figure 3**a shows the cyclic voltammogram (CV) of a rinsed $Na_{0.5}[Ni_{0.23}Fe_{0.13}Mn_{0.63}]O_2$ electrode. A series of peaks, associated with the electrochemical processes involving phase transformation occurring during the Na-extraction and insertion are observed. At lower voltage values, a pairs of reversible peaks at about 2.0V *vs.* Na/Na$^+$, probably associated with the $Mn^{4+}/Mn^{3+}$ redox process and the consequent structural rearrangement of the layers, [31,32] are detected. The additional peaks between 3.2 V and 3.9 V *vs.* Na/Na$^+$ can be attributed to the $Ni^{2+}/Ni^{4+}$ redox couple, with a double-electron process involving changes in the layers alignment in the material. At voltages higher than 4.2V, where the material contains a very low amount of sodium, a two-phase oxidation reaction associated with the formation of the O2-phase, resulting from the gliding of the layers without any change of the oxygen-transition metal bonds, is revealed by the CV trace.[19,21] This phase transition may be associated with residual $Ni^{3+}/Ni^{4+}$ oxidation as proposed in the literature.[33] The reverse reduction scan shows only the lower voltage peak, suggesting that the high voltage processes occur in a single step. This interpretation is supported by the comparison of the charge and discharge peak areas that, giving similar values, also confirms the reversibility of the reaction. As expected, the phase transitions and the structural reorganization above mentioned reflect in changes in the voltammetric profile of Fig.3a, where, during the first few cycles, the height of the highest voltage peak progressively decreases while its width increases. However, it is to be noticed that the peak stabilization is achieved upon cycling.

Figure 3b, reporting the coupled thermogravimetric–mass spectrometry analysis of $Na_{0.5}[Ni_{0.23}Fe_{0.13}Mn_{0.63}]O_2$, shows that the overall 4.5% weight loss up to 900°C is associated in minor part with the initial removal of water and release of $CO_2$, most likely due to the $NaHCO_3$ impurities decomposition occurring between 100°C and 300°C, and the $CO_2$ release at around 600°C, due to the decomposition of sodium carbonate impurities. It is important to notice that the material carbonate content is comparable with those commonly reported in the literature, i.e., of the order of 5% as indicated by TGA-MS.[23] The major weight loss,

however, is observed at temperatures higher than 300°C, which is associated with $O_2$ release from the layered structure promoted by heating in the oxygen-deficient atmosphere. Taking into account the rather high temperature corresponding to the $O_2$ evolution and the relatively low corresponding weight loss, about 2%, the $Na_{0.5}[Ni_{0.23}Fe_{0.13}Mn_{0.63}]O_2$ material here reported can be considered as a safe material in view of eventual thermal runaway of the sodium ion battery using it as the positive electrode.

Figure 4

The suitability of $Na_{0.5}[Ni_{0.23}Fe_{0.13}Mn_{0.63}]O_2$ as an effective cathode in sodium cells has been further confirmed by galvanostatic cycle tests in the 4.6V -1.5V range at various current regimes. **Figure 4** illustrates the voltage profiles and the cycling behavior of the sodium cell cycled at 15 mA $g^{-1}$ (a, b), 50 mA $g^{-1}$ (c, d) and 100 mA $g^{-1}$ (e, f), corresponding to a rate of about C/10, C/3 and C/2, respectively. As it is seen in the figure, the material is capable to deliver capacities ranging from 200 mAh $g^{-1}$ at the lowest current (Fig.4a) to 150 mAh $g^{-1}$ at the highest current (Fig.4e). These rather high values are, indeed, matching those expected by a structurally optimized, P2-type layered cathode. The enhanced cycle life, high charge-discharge efficiency and well-defined voltage plateau show the typical signature of a solid-solution intercalation process at lower voltages and a reversible phase transition at the higher voltages. These are all evidences confirming that the coexistence in the material of the different metals, i.e., Ni and Fe, effectively leads to the desired stabilization of the P2 phase. Finally, electrochemical impedance tests performed during cycling (see SI, Fig. S2) show a very stable behavior of the electrode impedance with typical changes associated to the formation and partial dissolution of the SEI film, suggesting for the formation of an optimized electrode-electrolyte interphase. However, it is important to point out that a minor decay associated with the high voltage, P2-O2 phase transition, resulting in the material structural

reorganization, still occurs. Work is in progress in our laboratories to fully understand and address this issue.

Figure 5

**Figure 5** reports the cycling response (a) and the voltage profile (b) of $Na_{0.5}[Ni_{0.23}Fe_{0.13}Mn_{0.63}]O_2$ upon galvanostatic cycle tests at increasing current rates (from C/10 up to 5C). The figure shows that the material delivers capacities ranging from 180 mAh $g^{-1}$ at C/10 to 60 mAh $g^{-1}$ at 5C, with high cycling efficiency, approaching 99% over the entire test. These results give a clear evidence of a rather fast kinetics of the sodium insertion/extraction electrode process. Furthermore, the almost complete recovery of the initial material capacity, reducing the current to the initial value of C/10 (see Fig. 5a), gives a further proof of the electrode stability. Indeed, a capacity retention of 95.3% is obtained comparing the discharge capacities delivered at the $10^{th}$ (175.9 mAh $g^{-1}$) and $40^{th}$ (167.6 mAh $g^{-1}$) cycles, although a stressful C-rate test (up to 5C) was applied. The voltage profiles confirm that the material operates with the expected trend up to a rate as high as 1C. Then, at higher C-rates, i.e. 2C and 5C, some additional polarization effects, quite likely due to electrolyte diffusion overvoltage, are observed. It is expected that the rate capability of the electrode may be improved reducing the particle size and enhancing the electrode morphology. Work is in progress in our laboratories to confirm this expectation. Certainly, additional tests focused on the study of the cut-off voltage effect on the cycle cell life may be helpful to fully understand and, hopefully optimize, the material characteristics. However, the consistent results so far obtained suggest $Na_{0.5}[Ni_{0.23}Fe_{0.13}Mn_{0.63}]O_2$ as an effective cathode for sodium batteries.

## 3. Conclusion

In this work we synthesized a $Na_{0.5}[Ni_{0.23}Fe_{0.13}Mn_{0.63}]O_2$ layered material characterized by a well defined P2-type structure. The optimized synthetic route, involving co-precipitation,

annealing and water-rinsing, resulted in the enhanced electrochemical behavior of the material in sodium cells, both in terms of cycling response and delivered capacity, which is extending up 200 mAh g$^{-1}$. Hence, the P2-type Na$_{0.5}$[Ni$_{0.23}$Fe$_{0.13}$Mn$_{0.63}$]O$_2$ layered electrode is here proposed as a suitable and efficient cathode for sodium-ion batteries.

## 4. Experimental Section

*Sample synthesis and characterization*

Na$_{0.5}$[Ni$_{0.23}$Fe$_{0.13}$Mn$_{0.63}$]O$_2$ was synthetized by a solid-state reaction between sodium hydroxide (NaOH pellets Sigma Aldrich > 98%) and nickel-iron-manganese precursor. The precursor was prepared by co-precipitation method. Stoichiometric proportions (0.2:0.1:0.7) of NiSO$_4$·6H$_2$O (Sigma Aldrich, ACS reagent 99%), FeSO$_4$·7H$_2$O (Sigma Aldrich, ACS reagent ≥99%), and MnSO$_4$·5H$_2$O (Sigma Aldrich, ACS reagent ≥98%) were used as the starting materials for the synthesis. An aqueous solution of the three sulfates (with a concentration of 0.1mol L$^{-1}$) was made by stirred till complete dissolution, resulting in a green coloration. A NaOH aqueous solution (50% excess) was added drop-wise in order to obtain the precursor. After extensive washing with a NH$_4$OH solution (aq. chelating agent in order to avoid eventual metal dissolution), the precipitate precursor [Ni$_{0.2}$Fe$_{0.1}$Mn$_{0.7}$](OH)$_2$ was dried over night at 70°C in an oven. After grinding, the powdery precursor was dried under vacuum at 130°C for 6 hours.

NaOH and the dried precursor [Ni$_{0.2}$Fe$_{0.1}$Mn$_{0.7}$](OH)$_2$ were dry-mixed with a mole ratio of 1:1. The mixture was annealed in air atmosphere at 500°C for 5 hours (5°C/min) and then, as pellet, at 800°C for 6 hours (heating rate: 5°C/min). Finally, the material was subjected to a water treatment in order to remove the excess of sodium and other soluble components. This was performed by stirring one gram of material in 100 mL of distilled water at 25°C for 5 min and then filtered.[23] Finally, the material was dried at 120°C for 24 hours, then ground and stored under inert atmosphere.

The sodium and transition metal ratios in the pristine and water-rinsed samples were detected by inductively coupled plasma optical emission spectrometry with a Spectro ARCOS ICP-OES (Spectro Analytical Instruments, Kleve, Germany) instrument with axial plasma viewing.

X-ray diffraction (XRD, Bruker D8 Advance, Germany) using the Cu Kα radiation in the 2θ range from 10° to 90° was used to determinate the crystalline structure. Morphological investigation of the samples was made using field emission scanning electron microscopy (FE-SEM, Zeiss Auriga).

*Electrochemical characterization*

Electrodes were prepared by mixing the active material (85 wt.%) with carbon black (10 wt.%, Super C65, TIMCAL) and polivinylidenedifluoride, PVdF, (5 wt.%, 6020 Solef, Arkema Group). The slurry was made adding an appropriate amount of N-methyl-2-pyrrolidone (NMP). After 2 hours of intimate mixing, the resulting slurry was cast onto Al foil and dried at 120 °C. Punching and pressing of disk electrodes (12 mm diameter) followed. The mass loading of the electrodes was around 3 mg cm$^{-2}$ (2.55 mg cm$^{-2}$ active material).

Sodium metal was used as counter and reference electrodes. The sodium was cut from sodium pieces (99.8%, Acros Organics), which were pressed and finally punched on the current collector.

The electrodes were assembled into Swagelok-type cells with 1M $NaPF_6$ in PC as electrolyte solution. The cells were cycled galvanostatically at different current rates between 4.6V and 1.5V at 20°C using Maccor series 4000 battery tester (U.S.A). The nominal material capacity, corresponding to 0.5 equivalent of Na per mole of material, is 143 mAh g$^{-1}$.

**Supporting Information**
Supporting Information is available from the Wiley Online Library or from the author.

[1]     N.-S. Choi, Z. Chen, S.A. Freunberger, X. Ji, Y.- K. Sun, K. Amine, G. Yushin, L.F. Nazar, J. Cho and P. G. Bruce, *Angew. Chem. Int*. Ed. **2012**, *51*, 9994-10024.

[2]     M. R. Palacin, *Chem. Soc. Rev* **2009**, *38*, 2565-2575.

[3]     B. Scrosati, J. Hassoun, Y.-K. Sun, *Energy Environ. Sci.* **2011**, *4*, 3287-3295.

[4]     B. W. Jaskula, Lithium, in Mineral Commodity Summaries **2012**, U. S. Geological Survey, Reston, VA, 2012, p. 94.

[5]     S. Fletcher, Bottle Lightning: Superbatteries, Electric Cars and the New Lithium Economy, Hill and Wang, New York, **2011**; B. Scrosati *Nature*, **2011**, *473*, 448.

[6]     S.-W. Kim, D.-H. Seo, X. Ma, G. Ceder and K. Kang, *Adv. Energy Mater* **2012**, *2*, 710-721.

[7]     V. Palomares, P. Serras, I. Villaluenga, K.B. Hueso, J. Carretero-González and T. Rojo, *Energy Environ. Sci*. **2012**, *5*, 5884-5901.

[8]     M. D. Slater, D. Kim, E. Lee and C. S. Johnson, *Adv. Funct. Mater.* **2013**, *23*, 947–958.

[9]     C. Delmas, C. Fouassier and P. Hagenmuller, *Physica* **1980**, *99*, 8-85.

[10]   C. Delmas, J- J. Braconnier, C. Fouassier, P. Hagenmuller *Solid State Ionics*, **1981,** *3/4*, 165-169.

[11]   R. Berthelot, D. Carlier, C. Delmas *Nat. Mater.* **2011**, *10*, 74-80.

[12]   S. Komaba, C. Takei, T. Nakayama, A. Ogata, N. Yabuuchi, *Electrochem. Comm.* **2010**, *12*, 355-358.

[13]   J. Zhao, L. Zhao, N. Dimov, S. Okada and T. Nishidac, *J. Electrochem. Soc.* **2013**, *160*, A3077-A3081.

[14]    N. Yabuuchi, H. Yoshida and S.Komaba, *Electrochemistry* **2012**, *80*, 716-719.

[15]    X. Ma, H. Chen, G. Ceder*, J. Electrochem. Soc*. **2011**, *158*, A1307-A1312.

[16]    C. Delmas, Y.  Borthomieu, C. Faure, *Solid State Ionics* **1989**, *32/33*, 104-111.

[17]    S. Komaba, N. Yabuuchi, T. Nakayama, A. Ogata, T. Ishikawa and I. Nakai, *Inorg. Chem.* **2012**, *51*, 6211-6220.

[18]    S.-M. Oh, S.-T. Myung, M.-W. Jang, B. Scrosati, J. Hassoun, Y.-K. Sun, ***Phys. Chem. Chem. Phys.*** **2013**, *15*, 3827-3833.

[19]    Z. Lu, J. R  Dahn, *J. Electrochem. Soc.* **2001**, *148*, A1225-A1229.

[20]    D. Carlier, J. H. Cheng, R. Berthelot, M. Guignard, M. Yoncheva, R. Stoyanova, B. J. Hwang, C. Delmas, *Dalton Trans.* **2011**, *40*, 9306-9312.

[21]    D. H. Lee, J. Xu and Y. S. Meng, *Phys. Chem. Chem. Phys.* **2013**, *15*, 3304-3312.

[22]    M. Sathiya, K. Hemalatha, K. Ramesha, J.-M. Tarascon and A. S. Prakash, *Chem. Mater.* **2012**, *24*, 1846-1853.

[23]    D. Buchholz, A. Moretti, R. Kloepsch, S. Nowak, V. Siozios, M. Winter and S. Passerini, *Chem. Mater.* **2013**, *25*, 142-148.

[24]    L.G.Chagas, D. Buchholz, L. Wu, B. Vortmann, S. Passerini, *J. Power Sources* **2014**, *247*, 377-383.

[25]    N. Yabuuchi, M. Kajiyama, J. Iwatate, H. Nishikawa, S. Hitomi, R. Okuyama, R. Usui, Y. Yamada and S. Komaba *Nat. Mate* **2012**, *11*, 512-517.

[26]    D. Kim, E. Lee, M. Slater, W. Lu, S. Rood, C.S. Johnson, *Electrochem. Comm.* **2012**, *18*, 66-69.

[27]    J. M. Paulsen and J. R. Dahn, *J. Electrochem. Soc.* **2000**, *147*, 2478-2485.

[28]    S.H. Kang; C.S. Johnson, J.T. Vaughey, K. Amine, M.M. Thackeray, *J. Electrochem. Soc.* **2006**, *153*, A1186-A1192.

[29]    J. Li, R. Kloepsch, M. Kunze, M. Winter, S. Passerini, *J. Power Sources* **2011**, *196*, 7687-7691.

[30]   Y. Wang, Y. Ding, J. Ni, *J. Phys. Condens. Matter* **2009**, *21*, 035401.

[31]   D. Yuan, W. He, F. Pei, F. Wu, Y. Wu, J. Qian,Y. Cao, X. Ai and H. Yang, *J. Mater. Chem. A* **2013**, *1*,3895-3899.

[32]   J.S. Thorne, R.A. Dunlap and M.N. Obrovac, *J. Electrochem. Soc.* **2013**, *160*, A361-A367.

[33]   D. Yuan, X. Hu, J. Qian,  F. Pei, F. Wu, R. Mao, X. Ai, H. Yang, Y. Cao, *Electrochimica Acta* **2014**, *116*,  300-305.
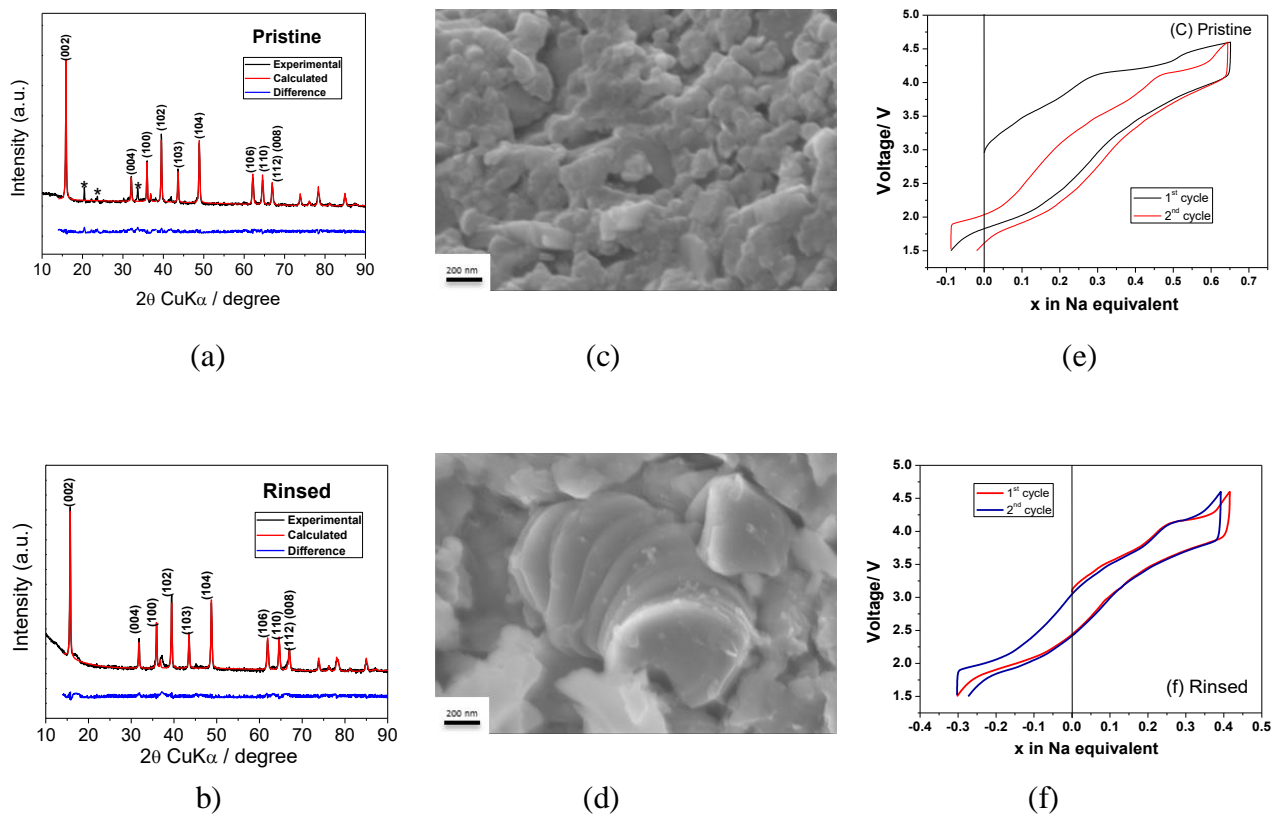
**Figure 1.** Experimental (black line) and calculated (red line) XRD diffraction pattern of the pristine (a) and rinsed (b) materials. Scanning electron microscopy images of the pristine (c) and rinsed (d) material. Voltage vs. composition profile (first and second charge/discharge curves) recorded during the galvanostatic test of the pristine (e) and rinsed (f) materials. Current rate of 15 mAg$^{-1}$. The insets in panels e and f illustrate the molar fraction (x) of Na reversibly (de-)inserted upon a few cycles.
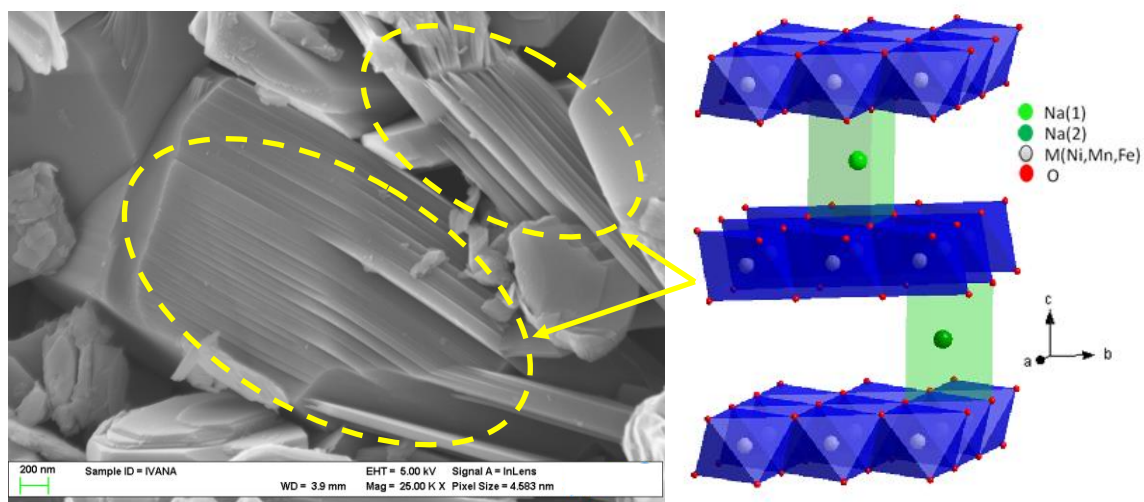
**Figure 2.** FE-SEM image of the rinsed material. A schematic illustration of the material structure as obtained by the refined cell parameters of Table 1 is also illustrated.
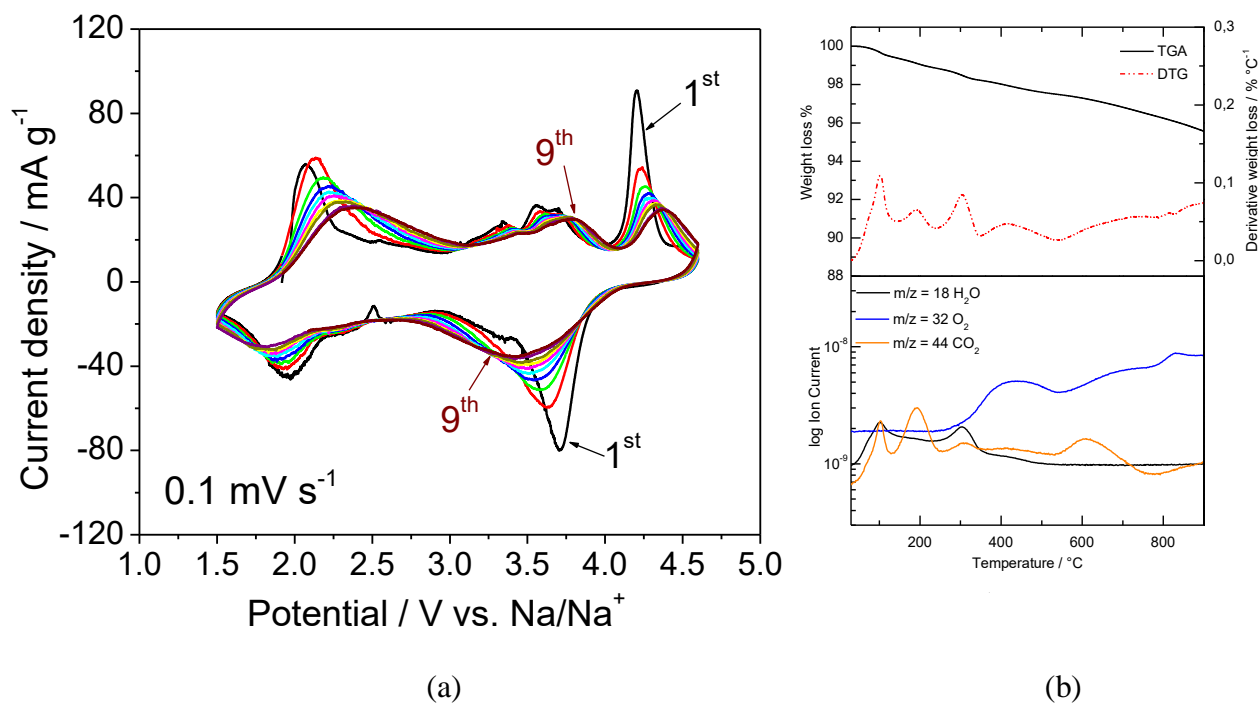
(a)

(b)

**Figure 3.** (a) Cyclic voltammogram of $Na_{0.5}[Ni_{0.23}Fe_{0.13}Mn_{0.63}]O_2$ performed at a scan rate of 0.1 mV s⁻¹ in the 4.6V-1.5V (*vs* Na/Na⁺) voltage range at 20°C±2°C ; (b) TGA-MS results for the rinsed material under He flux performed with a heating rate of 10K/min.
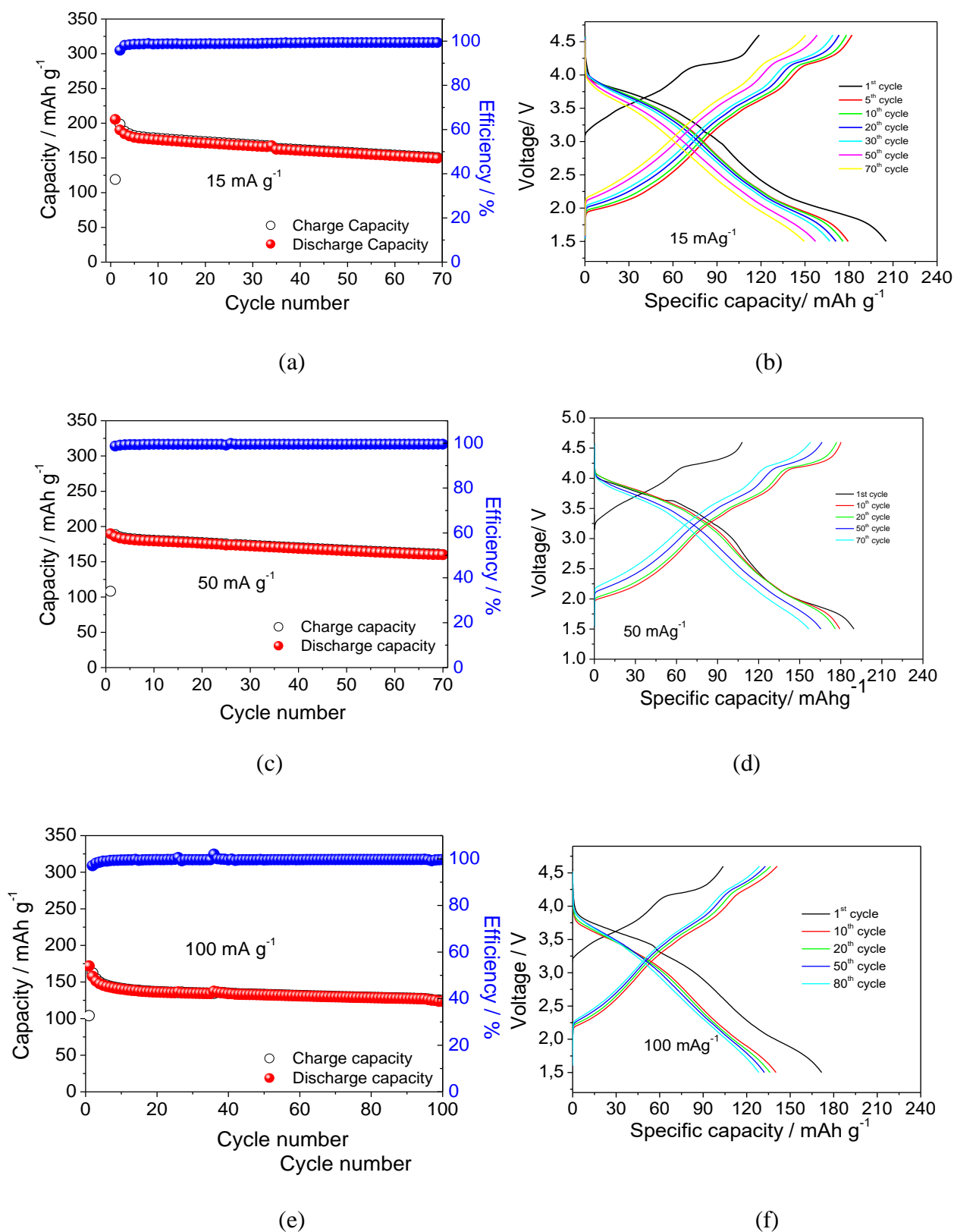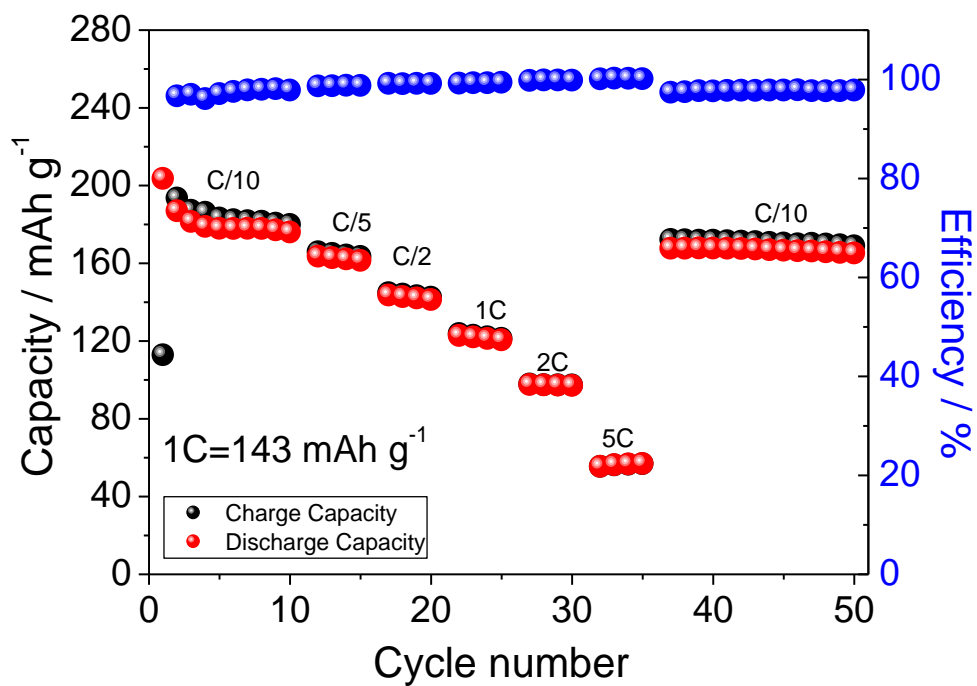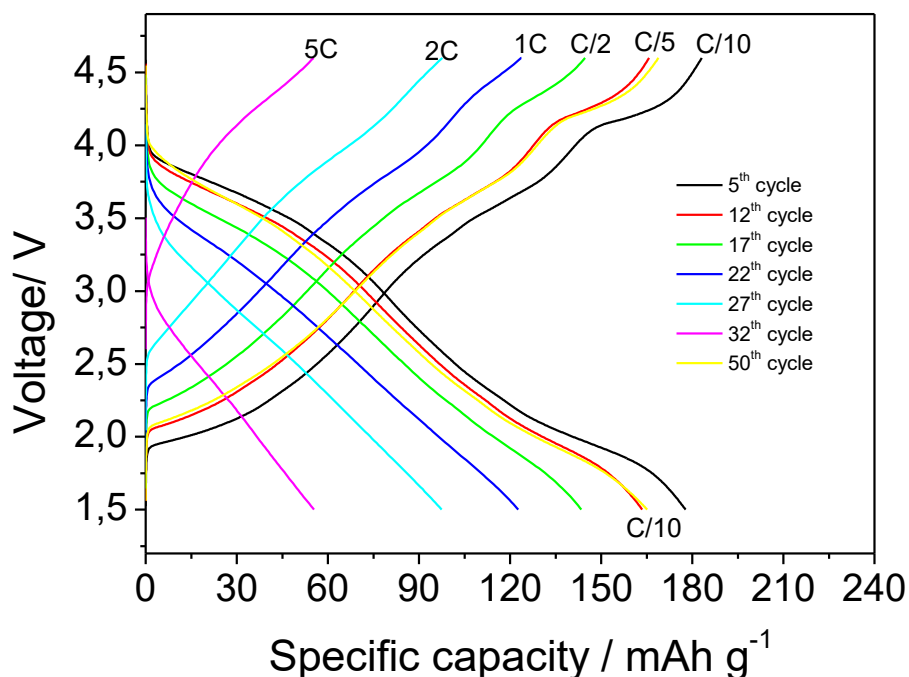
**Figure 4.** Performance of a Na / PC, NaPF$_6$ 1M / Na$_{0.5}$[Ni$_{0.23}$Fe$_{0.13}$Mn$_{0.63}$]O$_2$ cell upon galvanostatic charge–discharge cycles within the 4.6V–1.5V voltage range at 20°C ±2°C. The voltage profiles (a, c, and e) and cycling behavior (b, d, and f) are reported at various current rates (a and b: 15 mA g$^{-1}$; c and d: 50 mA g$^{-1}$; f and e: 100 mA g$^{-1}$).

(a)



(b)

**Figure 5.** Rate capability plot showing the performance at various rates of a Na / PC, NaPF$_6$ 1M / Na$_{0.5}$[Ni$_{0.23}$Fe$_{0.13}$Mn$_{0.63}$]O$_2$ cell in terms of delivered capacity (a) and voltage profiles (b). 1C current rate corresponds to 143mA g$^{-1}$. Temperature: 20°C±2°C.

**Table 1.** Structural characteristic and Rietveld refinement parameters of pristine and rinsed material.

|  | PRISTINE | RINSED |
|---|---|---|
| Lattice | hexagonal | Hexagonal |
| Space group | $P6_3/mmc$ | $P6_3/mmc$ |
| a (Å) | 2.88658(30) | 2.87986(14) |
| c (Å) | 11.1770(13) | 11.21716(50) |
| $V(\text{Å}^3)$ | 80.653(19) | 80.566(95) |
| Rwp | 7.10 | 5.46 |
| GOF | 2.52 | 2.26 |

…

The table of contents entry

A $Na_{0.5}[Ni_{0.23}Fe_{0.13}Mn_{0.63}]O_2$, P2-type electrode is synthesized by co-precipitation, annealing and water-rinsing and characterized in sodium cell. The electrode shows an enhanced cycling response delivers a capacity as high as 200 mAh $g^{-1}$. The P2-type, layered material is proposed as a suitable cathode for sodium batteries .

**Keyword**

$Na_{0.5}[Ni_{0.23}Fe_{0.13}Mn_{0.63}]O_2$, P2-type, layered, cathode, sodium-ion, battery

Ivana Hasa, Daniel Buchholz, Stefano Passerini[*], Bruno Scrosati and Jusef Hassoun[*]

**Title**

High performance $Na_{0.5}[Ni_{0.23}Fe_{0.13}Mn_{0.63}]O_2$ cathode for sodium-ion battery

ToC figure